Fabrication of kesterite absorber films by spray pyrolysis: Effect of annealing temperature on the phase formation

P. Prabeesh, P. Saritha, I Packia Selvam, S. N. Potty*

Centre for Materials for Electronics Technology (C-MET), Under Ministry of Electronics & Information Technology, Government of India, Shoranur Road, Athani PO, M.G Kavu, Thrissur, 680581, India

*Corresponding author, Tel: (+91) 487 2201156; Fax: (+91) 487 2201347; E-mail: snpotty@cmet.gov.in

Received: 30 March 2016, Revised: 27 September 2016 and Accepted: 30 November 2016

DOI: 10.5185/amp.2017/111
www.vbripress.com/amp

Abstract

Kesterite thin films have been fabricated by chemical spray pyrolysis technique using less toxic organic solvent followed by annealing at different temperatures in inert nitrogen atmosphere. Phase formation and structural evolution were studied by XRD and Raman spectroscopy. The films annealed at 450°C and 500°C exhibited excellent properties required for photovoltaic absorber materials. UV-Vis spectroscopy was used to estimate absorption coefficient and band gap; the films annealed at 450°C and 500°C showed band gap of 1.65eV and 1.51eV, respectively. Surface morphological properties and film thickness were studied by FESEM and electrical properties by Hall measurement system. Films annealed at 500°C showed densely packed grains with thickness ~ 1.2μm. Electrical properties of the films annealed in nitrogen atmosphere were in good agreement with the values previously reported for CZTS thin films. Copyright © 2017 VBRI Press

Keywords: Spray pyrolysis, kesterite, XRD, Raman, FESEM.

Introduction

Kesterite (CZTS, Cu_2ZnSnS_4) is a chalcogen based absorber material for solar cell applications. Several groups have studied various aspects of this material in the past few years and this wide attention is mainly due to the abundance of its constituent elements in the earth's crust and also due to its excellent photovoltaic properties. Kesterite has optimum band gap of 1.5eV, large absorption coefficient ($>10^4 cm^{-1}$) and composed of earth abundant and no-toxic materials **[1]**. The first report on the development of this quaternary material was by Nitche et al via iodine vapor transport in 1966 **[2]**. Later, Ito and Nakazawa developed CZTS and verified its potential as a thin film absorber material in 1988 **[1]**. In the device point of view, Katagiri et al **[3]** fabricated CZTS solar cell with 0.66% efficiency in 1996 and with 6.7% efficiency in 2008. Since then, the efficiency has gone up and recently reached a breaking record of efficiency of 12.6% for CZTSSe solar cell **[4]**. It has to be noted that this highest efficiency reported is still far from the theoretical efficiency of 32.2% **[4,5]**. This difference may be due to the difficulty to prepare this quaternary compound in single phase.

Several physical and chemical methods are currently adopted to deposit CZTS material **[5]**. Compared to vacuum based techniques, chemical methods are more attractive because of its low cost, simplicity and the suitability for large area deposition. Among the chemical methods, spray pyrolysis is the easiest method for large area deposition. Nakayama and Ito reported the fabrication of sprayed films of Cu_2ZnSnS_4 for the first time in 1996 and the raw materials used were chlorides and the sulphur source, thiourea. They dissolved the precursors in deionised water and sprayed onto the substrate at a rate of 3ml/min, the substrate, soda lime glass, was placed 15cm above and then heated by a nichrome heater indirectly **[6]**. Later, several groups investigated the effects of different parameters, such as substrate temperature, pH of the solution, etc. In another report, Rodriez et al. deposited films using $CuCl_2$, $Zn(CH_3COO)_2.2H_2O$, $SnCl_4$, and $SC(NH_2)_2$ precursors and the deposition was performed in an $Ar/Ar+H_2$ atmosphere followed by annealing in sulphur environment **[7]**. Several groups reported the deposition of CZTS using chloride precursors and annealing in different sulphur environments. Tanaka et al reported annealing of the CZTS thin films by placing precursor films of Sn and S face to face during the annealing process to suppress the evaporation of S and Sn **[8]**. In the present study, precursor thin films were deposited at 350°C using zinc acetate, copper acetate, tin chloride and thiourea system and studied the effect of inert atmosphere annealing on phase formation and structural, optical and electrical properties of CZTS films. As far as the authors know, no work has been reported on the effect of organic solvent on the properties of spray pyrolysed CZTS absorber films.

Experimental

Materials

The precursor solution was prepared by dissolving copper (II) acetate monohydrate (emsure, 99-102%) (0.02M), zinc (II) acetate dehydrate (emsure, 99.5-101%)) (0.01M), tin (II) chloride (emsure, 98-103%) (0.01M) and thiourea (GR, 99%) (0.16M) into 2-methoxyethanol (emparta, 99.3%). All chemicals were purchased from Merck India and used without further purification.

Preparation of CZTS thin film

Precursor solution was prepared by using 2 methoxy ethanol as solvent and excess thiourea was added to the solution to compensate the possible sulphur evaporation during the preheating or annealing processes and this will also act as an oxidation inhibitor **[9]**. Glass substrates were ultrasonically cleaned with mild soap solution, distilled water, acetone and isopropyl alcohol for 15 min each and dried with free flow of nitrogen gas, before coating. Films were deposited by spraying the precursor solution on to the cleaned substrate at the rate of 8 mL/min. The substrate temperature was kept at 623 K throughout the process. Air blast atomizer containing pure nitrogen gas with flow rate of 4 L/min was used a carrier gas for the deposition. The distance between the spray nozzle and substrate was kept at 10 cm throughout the deposition and the deposited film was allowed to cool to room temperature. After the deposition, the films were annealed in nitrogen atmosphere for 30 min at different temperatures. **Fig. 1** shows the schematic diagram of the experimental set up used for annealing the precursor thin films.

Characterizations

Phase formation was confirmed with X-ray diffractometer (Bruker AXS D5005) and Raman spectroscope (Thermo scientific DXR Raman microscopy with 532 nm semiconductor LASER source). Surface morphological studies of the film were carried out using field emitting scanning electron microscope (FEI NOVA NANO SEM 450) and optical characterization by UV-Vis spectroscopy (Perkin Elmier: Lamda 35). Hall measurement set up (Ecopia HMS-3000) was used to study the electrical properties of the films.

Results and discussion

Fig. 2 shows the XRD patterns of as deposited and nitrogen annealed CZTS thin films. The as-deposited film did not show any peaks in the XRD pattern, indicating amorphous nature for the film.

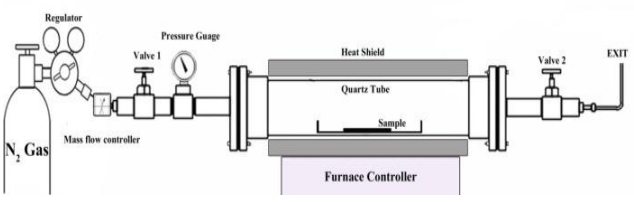

Fig. 1. Nitrogen annealing setup.

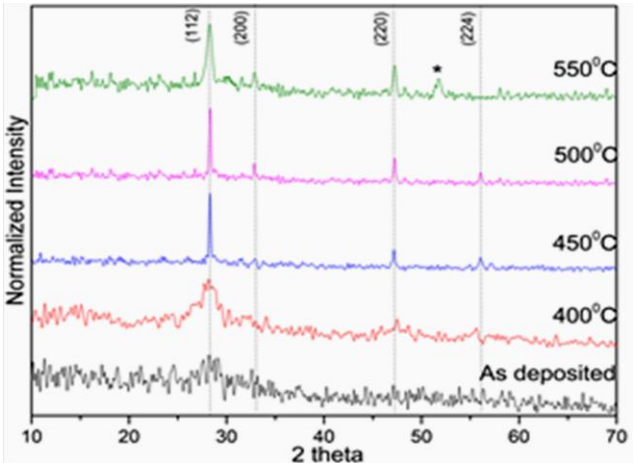

Fig. 2. XRD patterns of CZTS films annealed at different temperatures.

Two peaks were observed in the XRD pattern of the film annealed at 400°C, which corresponds to the planes (112) and (220) of kesterite phase. As seen in the XRD pattern, the film annealed at 450°C exhibited three peaks corresponding to CZTS (ICDD-PDF 26-0575). This indicates the formation of kesterite phase at 450°C. The film annealed at 500°C had relatively high intense peaks corresponding to (112), (200), (220), and (312) planes of kesterite**.** At 550°C, a peak corresponding to the impurity phase $Cu_{2-x}S_x$ was observed **[10]**. Annealing at high temperature may have resulted in the melting and subsequent evaporation of the film and which may be the reason for the appearance of secondary phase.

Lattice constants and crystalline size were estimated from the XRD patterns. Average crystalline size was calculated using Scherrer's formula **[11]**. **Table 1** shows the lattice parameters and average size of the CZTS films annealed at 450°C and 500°C. These values are in good agreement with the single crystal data, a = 0.5427nm and c = 1.0848nm (ICDD PDF No.26-0575). The crystal structure and size of CZTS thin films were found to vary with annealing temperature. Also, the peak width is narrowed with temperature. As seen in the figure, the peak intensity is found to increase with the increase in annealing temperature. Thus, the average particle size and the crystallinity of the particles were found to increase with the annealing temperature. It has been reported that the improvement in crystallinity of the absorber layer enhances the efficiency of solar cells **[8]**. In this study, the kesterite phase was formed at 450°C and the crystallinity was found to increase when the annealing temperature was increased to 500°C.

Table 1. Lattice parameter and average crystalline size of the films annealed at 450°C and 500°C.

Annealing temperature	*(hkl)*	*d* (A^0)	Lattice parameter (*nm*)		Crystalline size *(nm)*
			a=b	*c*	
500°C	112	3.14	0.543	1.08	45
	220	1.92			
450°C	112	3.15	0.544	1.09	42
	220	1.92			

It is difficult to confirm the exact formation of Cu_2ZnSnS_4 phase from X-ray diffraction measurements because of similar crystal structure possessed by other secondary phases such as ZnS and Cu_2SnS_3. To confirm the formation of single phase Cu_2ZnSnS_4, the films were further investigated by Raman spectroscopy.

Cu_2ZnSnS_4 has a space group of I4, primarily consists of two alternating cation layers each containing Cu and Zn atoms. Cu_2ZnSnS_4 contains 8 atoms per primitive cell and there are 24 vibrational modes, in which 15 Raman active modes exist for kesterite structure **[12]**. It includes A, B and E modes. A mode arises from the symmetric vibration of anions, B mode arise from the movement of cations along the z-direction and E mode from the motion of cations in the X-Y plane. Among these modes, B and E may lead to TO/LO splitting due to their polar character **[12]**.

Raman spectra of the films annealed at different temperatures are shown in **Fig 3**. The films annealed at 350°C and 400°C exhibited major peak of CZTS at 332 cm^{-1}. The film annealed at 450°C and 500°C showed peaks at 332 cm^{-1} and 286 cm^{-1}, which arises from the vibration of A mode **[13]**. No other peaks from binary or ternary secondary phases were observed. This indicates that phase pure nature of films at 450°C and 500°C. One major peak at 465 cm^{-1} was observed in the spectra of the film annealed at 550°C, which may be due to the phase $Cu_{2-x}S$ **[10]** and shoulder peak at 331 cm^{-1} corresponds to that of Cu_2ZnSnS_4, with a shift in the peak position. The XRD and Raman studies confirmed the formation of single phase kesterite films when annealed in inert atmosphere at 450°C and 500°C.

Fig. 4(a-d) shows FESEM micrographs of the films annealed at different temperatures from 400°C to 550°C. The grains and grain boundaries are clearly visible in the **Fig. 4(b, c)**. As seen, the surface morphology of the Cu_2ZnSnS_4 film is significantly affected by the post annealing treatment in inert atmosphere. The grain size is found to be very small at 450°C. However, the film annealed at 500°C showed densely packed grains with large grain size. Thus, a dense CZTS film with improved microstructure was formed at an annealing temperature of 500°C. **Fig. 4(e)** shows the cross section of film annealed at 500°C and the thickness of the film measured from the image was ~1.2 µm.

Optical properties of the films were studied using UV visible spectroscopy. The optical absorption coefficient α, of the film was calculated from the transmittance spectra. The energy band gap for direct band gap materials can be estimated using the well-known tauc relation,

$$(\alpha h\upsilon)^2 = A(h\upsilon - Eg)$$

where, α and hυ are the absorption coefficient and photon energy respectively, Eg is the energy band gap and A is an energy dependent quantity. The band gap energy was estimated by extrapolating the linear portion of the plot of $(\alpha h\upsilon)^2$ versus hυ to the x intercepting point at y=0 (inset of **Fig. 5**).

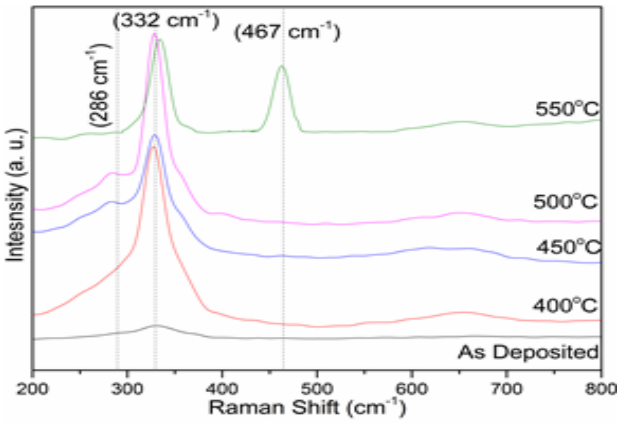

Fig. 3. Raman spectra of films annealed at different temperatures.

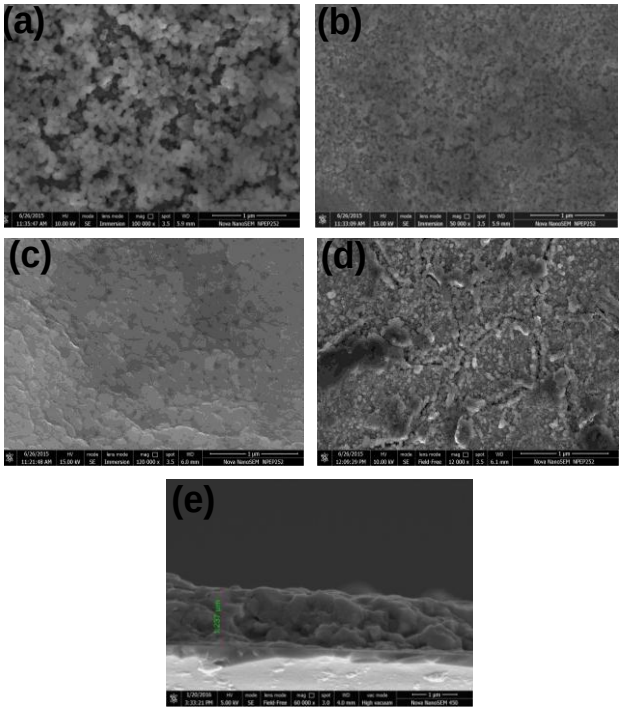

Fig. 4. FESEM images of the CZTS films annealed at (a) 400°C, (b) 450°C, (c) 500°C, (d) 550°C and (e) cross sectional image of CZTS film deposited at 500°C on SLG substrate.

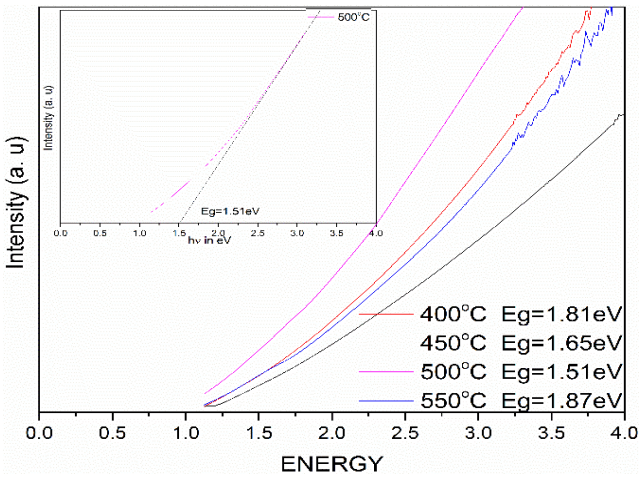

Fig. 5. $(\alpha h\upsilon)^2$ vs hυ plot (tauc plot) of the CZTS films annealed at different temperature.

Band gaps of the films were observed to be in the range 1.51-1.87 eV at room temperature, depending on the annealing temperature. The band gap decreases with increasing annealing temperature. The observed decrease in bandgap from 1.81 eV to 1.51 eV may be due to the improved crystallinity of the film **[14]**. The band gap is found to increase at higher temperatures, above 500°C, and this may be due to the formation of secondary phases in the films at this temperature. The secondary phase was observed in the XRD and Raman studies. The band gap was found to be ~1.51 eV for the film annealed at 500°C in nitrogen atmosphere. This value is close to the optimum band gap energy needed for thin film photovoltaic cell. The absorption coefficient (α) was found to be ~10^5 cm^{-1} in the visible region, the higher value indicates that it can absorb most of the incident photons with minimum thickness.

Table 2. Hall measurement data of CZTS thin films annealed at different temperature.

Annealing temperature	Carrier concentration /cm^3	Mobility cm^2/Vs	Resistivity Ωcm
350°C	4.299×10^{15}	47.04	30.86
400°C	2.128×10^{16}	40.24	18.07
450°C	5.147×10^{17}	33.94	0.36
500°C	2.368×10^{18}	12.03	0.22
550°C	8.448×10^{15}	100.4	73.62

Hall measurements were carried out in the present study to measure the electrical properties of the spray pyrolysed and nitrogen annealed Cu_2ZnSnS_4 films. The measurements were carried out in magnetic field intensity of 0.54 T. Hall measurements with van der Pauw configuration revealed a positive Hall coefficient, indicating *p* type nature of the films. Electrical properties of the films annealed at different temperature are summarized in **Table 2**. The carrier concentration was found to increase with annealing temperature while the mobility was found to decrease. This may be due to the improved crystallinity of the films at higher temperatures **[10, 15]**. The carrier concentration, mobility and resistivity of the films annealed at 500°C were observed to be 2.37×10^{18} cm^{-1}, 12 $cm^2V^{-1}S^{-1}$, and 0.22 Ωcm respectively. Similar results have been reported by Swami et al and Rajeshmon et al for spray pyrolysed film **[10, 16]**, Zhang et al and Tanaka et al for sputtered and sulphurized film (in N_2/Ar+S atmosphere) and Zhou et al for screen printed and argon annealed film **[17, 18, 19]**. The present study indicates that the non-vacuum and non-toxic process described in this work is suitable for deposition of phase pure CZTS thin films for photovoltaic applications.

Conclusion

Cu_2ZnSnS_4 absorber thin films were successfully fabricated through a simple and cost effective spray pyrolysis technique. An organic solvent was used for preparing the solution for the spray pyrolysis. X-ray diffraction, Raman spectroscopy, FESEM, UV-visible spectroscopy and Hall Effect measurements were carried out to characterize the spray pyrolysed film. The as-deposited films were annealed in nitrogen atmosphere at different temperatures ranging from 350°C to 550°C. Formation of phase pure Cu_2ZnSnS_4 was confirmed from the XRD patterns and Raman spectra. XRD analysis revealed the formation of kesterite phase at an annealing temperature of 450°C. However, crystallinity was found to increase when the annealing temperature was increased to 500°C. Raman spectra of the films did not indicate any secondary phases in the films annealed at 450°C and 500°C. The study indicated that the film annealed at 500°C possesses proper phase and crystallinity. The absorption co-efficient calculated from the UV-visible spectra was found to be ~10^5 cm^{-1} in the visible region and the optical band gap estimated was 1.51 eV for the films annealed at 500°C. Microstructure of the film annealed at 500°C exhibited a dense and improved grain structure. Hall measurements indicated *p* type nature for all the films. Hole concentration and resistivity of the films were found to be 2.37×10^{18} cm^{-3} and 0.22 Ωcm respectively. Thus, the Cu_2ZnSnS_4 absorber film fabricated using organic solvent through spray pyrolysis technique possesses the required photovoltaic properties.

Acknowledgements

Research grant received from Department of Science & Technology, Government of India (No.DST/TM/SERI/2K12/120) is gratefully acknowledged. Special thanks are due to Dr. R Ratheesh for helpful discussions in Raman Spectroscopy.

Author's contributions

Conceived the plan: SNP, PP: Performed the experiments: PP, PS, IPS, SNP; Data Analysis: PP, PS, IPS, SNP; Wrote the paper: PP, SNP: Authors have no competing financial interest.

References

1. Ito, K.; Nakazawa, T; *Jpn. J. Appl. Phys*., **1988**, *27*, 2094.
2. Nitsche, R.; Sargent, D. F.; Wild, P. J.; *Cryst. Growth*, **1967**, *1*, 52.
3. Katagiri, H.; Sasaguchi, N.; Hando, S.; Hoshino, S.; Ohashi, J; Yokota, T.; *Sol. Energy Mater. Sol. Cells*, **1997**, *49*, 407.
4. Wang, W.; Winkler, M.T.; Gunawan, O.; Gokmen, T.; Todorov, T. K.; Zhu, Y.; Mitzi, D. B.; *Adv. Energy Mater*., **2014**, *4*.
5. Bhosale, S. M.; Suryawanshi, M. P.; Kim, J. H.; Moholkar, A. V.; *Ceram. Int*., **2015**, *41*, 8299.
6. Nakayama, N.; Ito, K.; *Appl. Surf. Sci*., **1996**, *92*, 171.
7. Rodriguez, ME.; Sylla, D.; Sanchez, Y.; López-Marino, S.; Fontané, X.; López-García, J.; Placidi, M.; Pérez-Rodríguez, A.; Vigil-Galán, O.; Saucedo, E.; *J. Phys. D: Appl. Phys*., **2014**, *47*, 245101.
8. Tanaka, K.; Kato, M.; Goto, K.; Nakano, Y.; Uchiki, H.; *Jpn. J. Appl. Phys*., **2012**, *51*, 10NC26.
9. Aono, M.; Yoshitake, K.; Miyazaki, H.; *physica status solidi (c)*, **2013**, *10*, 1058.
10. Swami, S. K.; Chaturvedi, N.; Kumar, A.; Dutta, V.; *Sol. Energy*, **2015**, *122*, 508.
11. Cullity, B. D; Stock, S. R. (3rd); Elements of X-Ray Diffraction; Prentice-Hall Inc.: USA, **2001**.
12. Dimitrievska, M.; Fairbrother, A.; Fontané, X.; Jawhari, T.; Izquierdo-Roca, V.; Saucedo, E.; Pérez-Rodríguez, A.; *Appl. Phys. Lett.*, **2014**, *104*, 021901.
13. Kahraman, S.; Çetinkaya, S.; Podlogar, M.; Bernik, S.; Çetinkara, H. A.; Güder, H. S.*; Ceram. Int.*, **2013**, *39*, 9285.

14. Bodnar, I. V.; Telesh, E. V.; Gurieva, G.; Schorr, S.; *J. Electron Mater*., **2015**, *44*, 3283.
15. Prabeesh, P.; Packia Selvam, I.; Potty, S. N.; *Thin Solid Films*, 2016.
16. Rajeshmon, V. G.; Kartha, C. S.; Vijayakumar, K. P.; Sanjeeviraja, C.; Abe, T.; Kashiwaba, Y.; *Sol*. *Energy*, **2011**, *85*, 249.
17. Zhang, J.; Lexi, S. H.; Yujun, F.U.; Erqing; *Rare Metals*, **2006**, *25*, 315.
18. Tanaka, T.; Nagatomo, T.; Kawasaki, D.; Nishio, M.; Guo, Q.; Wakahara, A.; Yoshida, A.; Ogawa, H.; *J. Phys. Chem. Solids*, **2005**, *66*, 1978.
19. Zhou, Z.; Wang, Y.; Xu, D.; Zhang, Y.; *Sol. Energ. Mat. Sol. C*, **2010**, *94*, 2042.

